Supporting Information

Self-cascade MoS_2 nanozymes for efficient intracellular antioxidation and hepatic fibrosis therapy

Xinyu Zhang,[#a,b] Shitong Zhang,[b,#] Zaixing Yang,[b] Zhuanhua Wang,[*a] Xin Tian,[*b] and Ruhong Zhou[*b,c,d]

[a] *Institute of Biotechnology, Key Laboratory of Chemical Biology and Molecular Engineering of Ministry of Education, Shanxi University, Taiyuan 030006, China.*

[b] *State Key Laboratory of Radiation Medicine and Protection, School of Radiation Medicine and Protection, School for Radiological and Interdisciplinary Sciences (RAD-X), Collaborative Innovation Center of Radiation Medicine of Jiangsu Higher Education Institutions, Soochow University, Suzhou 215123, China*

[c] *Institute of Quantitative Biology, College of Life Sciences, Zhejiang University, Hangzhou 310058, China*

[d] *Department of Chemistry, Columbia University, New York, NY 10027, United States*

[#]These authors contributed equally to this work.

[*]Corresponding authors: E-mail: zhwang@sxu.edu.cn; xtian@suda.edu.cn; rz24@columbia.edu.

Other Methods

Electron spin resonance measurements

All electron spin resonance (ESR) measurements were carried out at ambient temperature using a Bruker E500 ESR spectrometer.

Measurement of CAT-like activity. Electron spin resonance (ESR) spin label oximetry was employed to investigate the oxygen generation from H_2O_2 catalyzed by MoS_2 nanosheets at two pH levels. Sample solutions including 0.1 mM spin label ^{15}N-PDT (Cambridge Isotope Labs, USA), 100 µg/mL MoS_2 nanosheets, and buffer solutions (pH 4.5 or 7.4) were deoxygenated with nitrogen before the initiation of reactions by addition of 1.0 mM H_2O_2. ESR spectral measurements were obtained using the following settings: 0.04 G field modulation, 3 G scan range, and 1 mW microwave power.

Measurement of SOD-like activity. To investigate the $O_2^{\bullet-}$ scavenging ability of MoS_2 nanosheets, two $O_2^{\bullet-}$ sources, xanthine-xanthine oxidase (XAN-XOD) and KO_2/18-crown-6-ether systems, were used to generate $O_2^{\bullet-}$. BMPO (Dojindo Laboratories, Japan) was used to trap the $O_2^{\bullet-}$ in the form of spin adduct BMPO/•OOH. ESR spectral measurements were obtained using the following settings: 1 G field modulation, 100 G scan range, and 20 mW microwave power.

Measurement of antioxidative effects of MoS_2 nanosheets through interaction with cytochrome c/H_2O_2. Oxidation of the spin trap DMPO (Dojindo Laboratories, Japan), to form 5,5-dimethyl-1-pyrrolidone-N-oxyl (DMPOX), was monitored by ESR to determine the effects of MoS_2 nanosheets on cytochrome *c* (Cyt *c*)'s ability to catalyze the oxidation of substrates by H_2O_2. Time dependence of the ESR signal for the Cyt *c*/H_2O_2 system with MoS_2 nanosheets or PBS (control) was measured. ESR spectral measurements were obtained using the following settings: 1 G field modulation, 100 G scan range, and 10 mW microwave power.

Table S1 Michaelis-Menten parameters of MoS_2 nanosheets.

Substrate	K_m (mM)	V_{max} (10^{-6} M s^{-1})	K_{cat} (10^{-3} s^{-1})	K_{cat}/K_m (10^{-3} mM^{-1} s^{-1})
H_2O_2	0.04	0.66	1.05	26.25
GSH	1.68	0.94	1.50	0.89

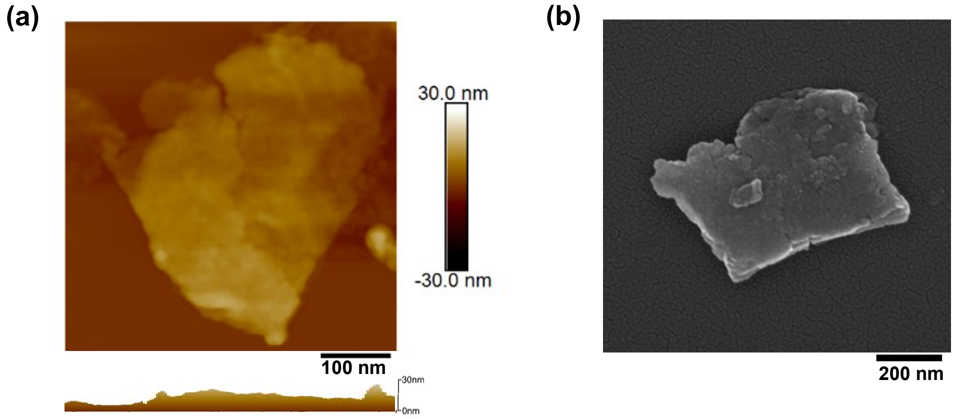

Fig. S1 (a) AFM and (b) SEM images of MoS_2 nanosheets.

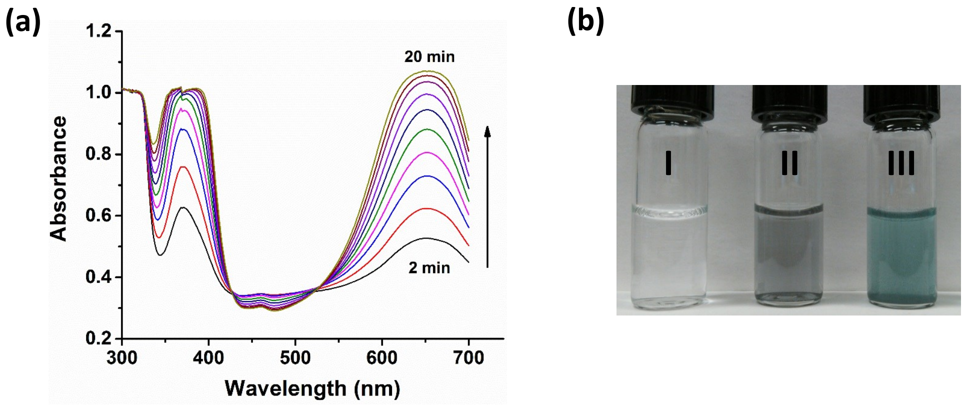

Fig. S2 (a) The absorbance spectra of TMB oxidized by MoS_2 nanosheets. (b) Typical photographs of TMB reaction solutions oxidized by MoS_2 nanosheets in the presence of H_2O_2 under pH 4.5. (I) 1 mM H_2O_2 and 1 mM TMB; (II) 100 μg/mL MoS_2 nanosheets and 1 mM TMB; (III) 1 mM H_2O_2, 1 mM TMB and 100 μg/mL MoS_2 nanosheets.

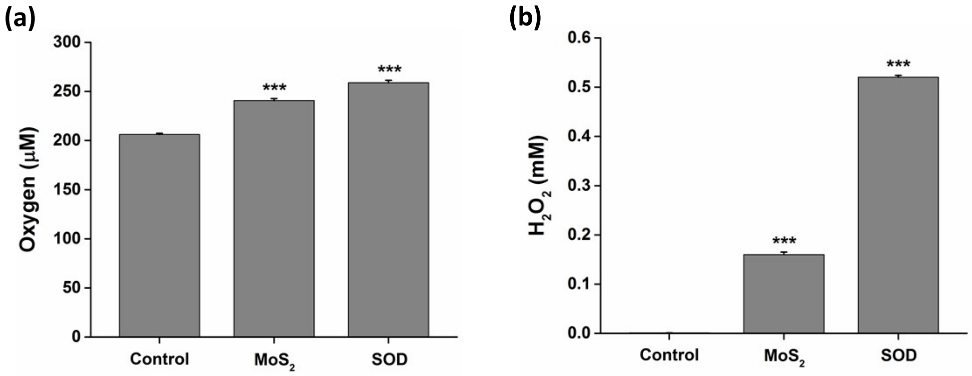

Fig. S3 The quantification of (a) oxygen and (b) H_2O_2 production from superoxide turnover by MoS_2 nanosheets *vs* 1 U/mL SOD in KO_2/18-crown-6-ether system. $^{***}p <$ 0.001 when compared with control group.

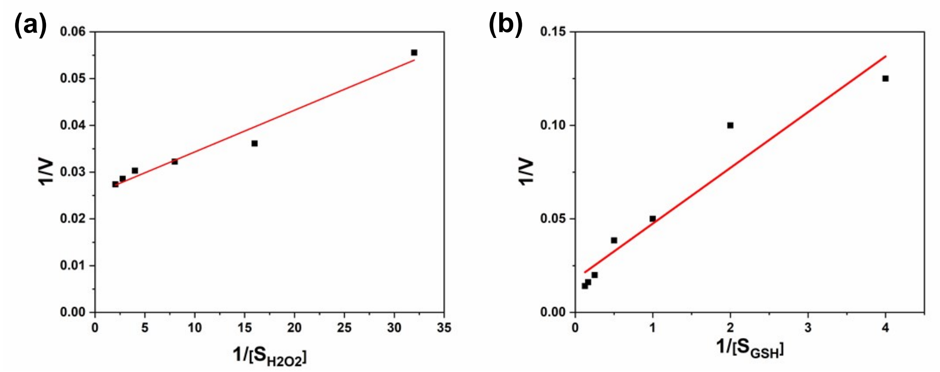

Fig. S4 Corresponding double-reciprocal plots of MoS_2 nanosheets at a fixed concentration of one substrate *versus* varying the concentration of another for (a) H_2O_2 and (b) GSH.

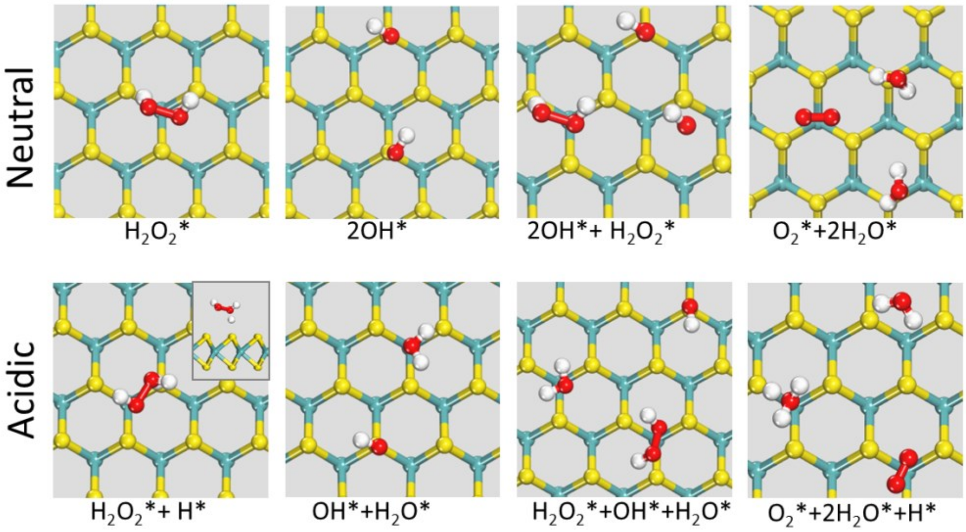

Fig. S5 Lowest-energy adsorption structures of the intermediate species during the H_2O_2 decomposition process on the basal plane of the MoS_2 nanosheets under neutral (top panel) and acidic (bottom panel) conditions (white, H; red, O; yellow, S; cyan, Mo).

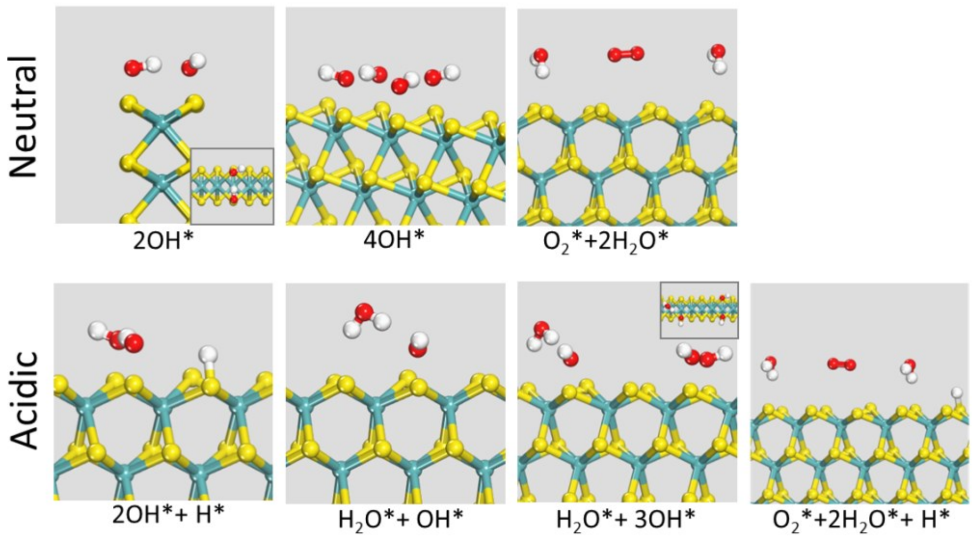

Fig. S6 Lowest-energy adsorption structures of the intermediate species during the H_2O_2 decomposition process on the Mo-S-edge of the MoS_2 nanosheets under neutral (top panel) and acidic (bottom panel) conditions (white, H; red, O; yellow, S; cyan, Mo). Here, it is noteworthy that the adsorption of H_2O_2 on Mo-S-edge is a chemical dissociative adsorption.

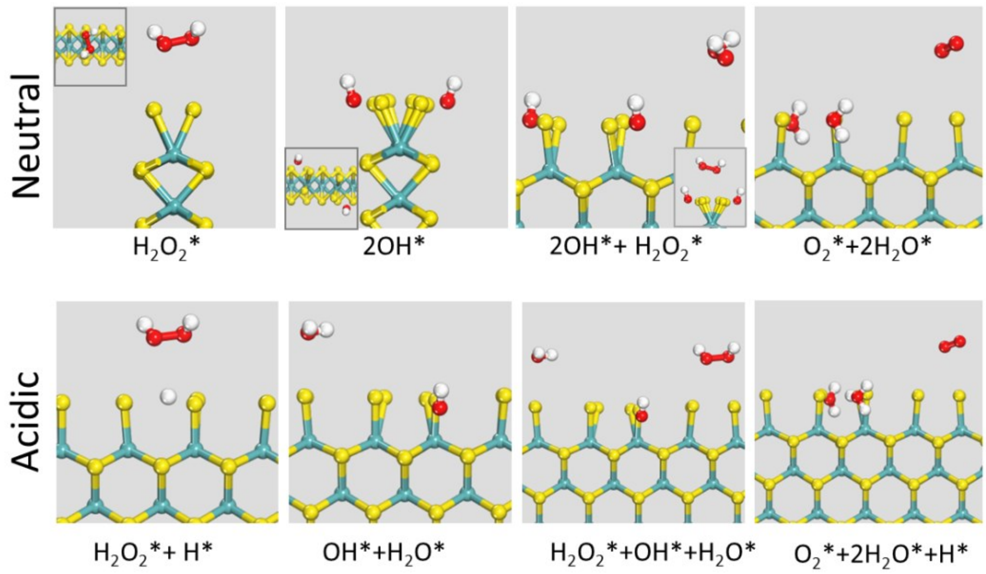

Fig. S7 Lowest-energy adsorption structures of the intermediate species during the H_2O_2 decomposition process on the S-edge of the MoS_2 nanosheets under neutral (top panel) and acidic (bottom panel) conditions (white, H; red, O; yellow, S; cyan, Mo).

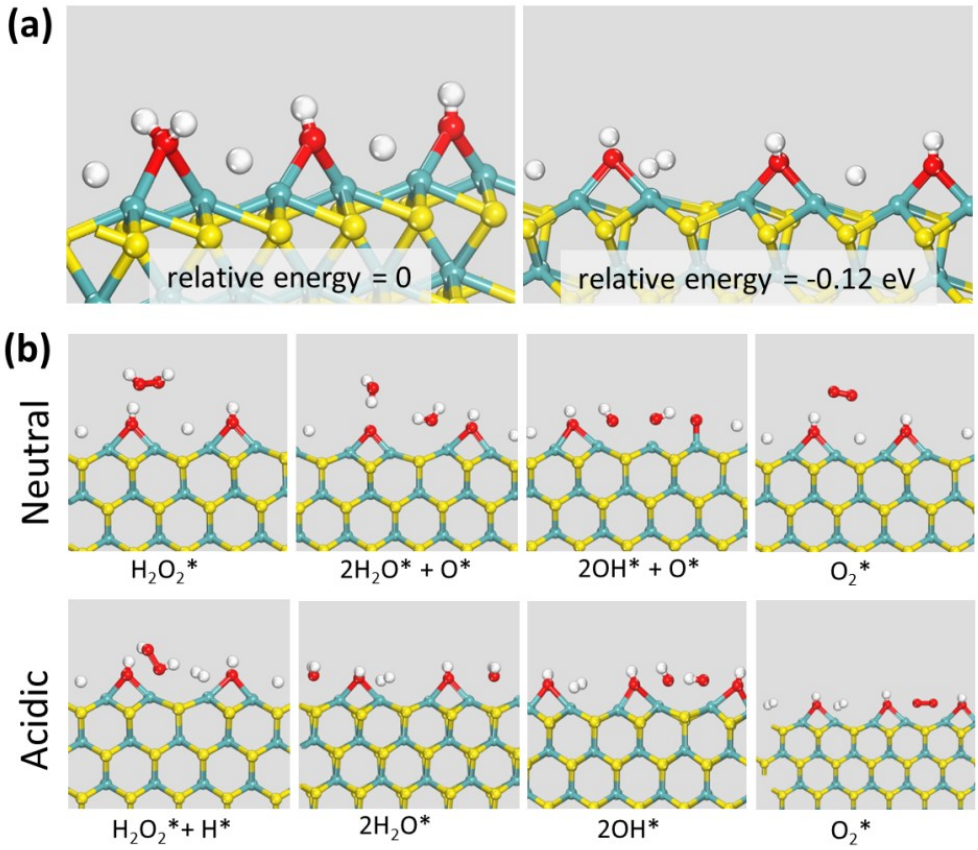

Fig. S8 (a) Comparison between two stable adsorptions of H^+ on the Mo-edge; the adsorption at the H-site is more energetically stable. (b) Lowest-energy adsorption structures of the intermediate species during the H_2O_2 decomposition process on the Mo-edge of the MoS_2 nanosheets under neutral (top panel) and acidic (bottom panel) conditions (white, H; red, O; yellow, S; cyan, Mo).

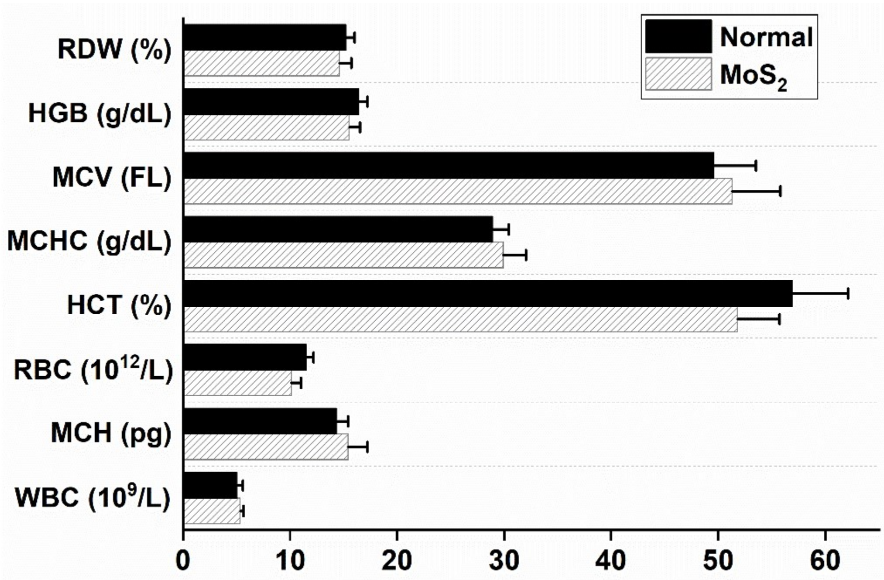

Fig. S9 Blood hematology data of mice injected with saline (normal group) or MoS_2 nanosheets (0.5 mg/kg.bw) once a week for four weeks.